Supplementary Information

Spontaneously amplified homochiral organic-inorganic nano-helix complex via self-proliferation

Halei Zhai[a] , Yan Quan[a], Li Li[a], Xiang-Yang Liu[b], Xurong Xu[c] and Ruikang Tang*[a,c]

[a] Centre for Biomaterials and Biopathways and Department of Chemistry, Zhejiang University, Hangzhou, 310027, China.

[b] Department of Physics and Department of Chemistry, National University of Singapore, Singapore 117542, Singapore.

[c] Qiushi Academy for Advanced Studies, Zhejiang University, Hangzhou, Zhejiang 310027, China.

1. Supporting figures

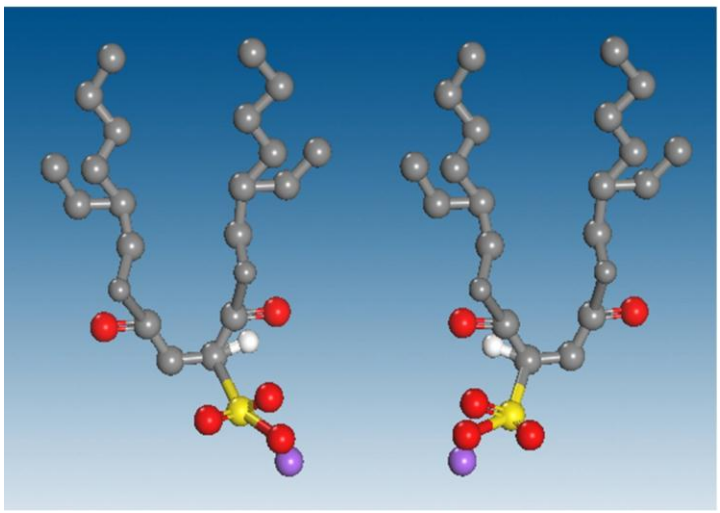

Fig. S1. Schematic structure of L (left) and R (right) formed AOT molecules. The chirality here only referred the carbon atom linked with $-SO_3^-$ groups. Gray: Carbon atoms. Red: Oxygen atoms. Yellow: sulphur atoms. Purple: sodium ions. The hydrogen atoms linked with chiral carbon atom (white) were specifically noted. Note: AOT itself is very difficult to purify the racemic mixtures. We simplify the racemic mixture to be L- or R- form according to the resulted L- or R- helix.

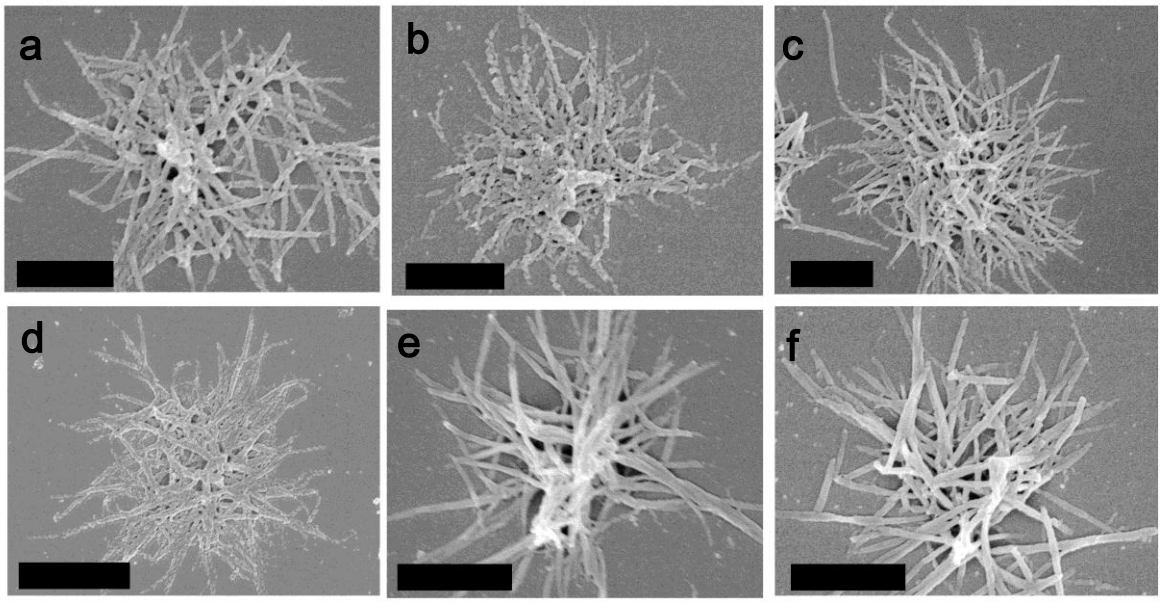

Fig. S2. Homochiral helix clusters. a-c) L-handed, and d-f) R-handed. Bar= 1 μm.

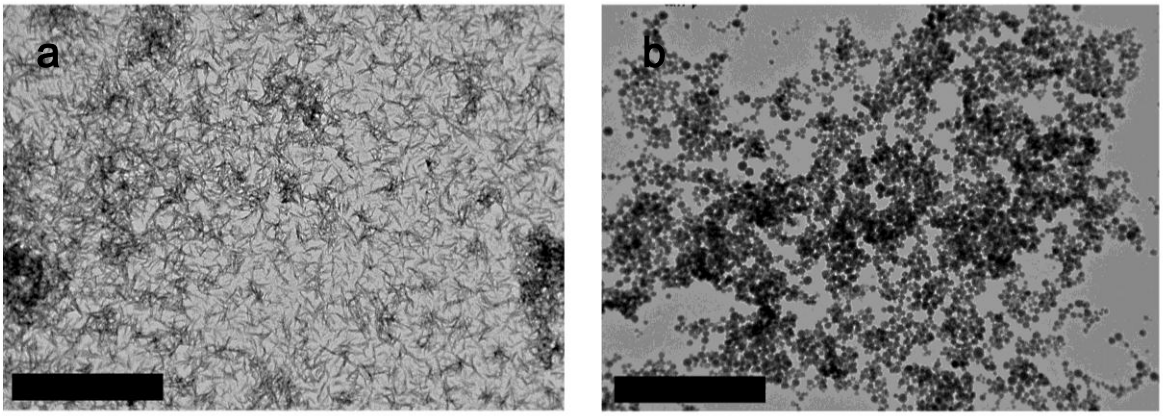

Fig. S3. a) The formed HAP nanoparticles by using AOT alone. b) Poor crystalline calcium phosphate nanoparticles by using BSA alone. Note: various concentrations of AOT and BSA alone were tested but the hybrid helixes failed to form. Bar= 2μm.

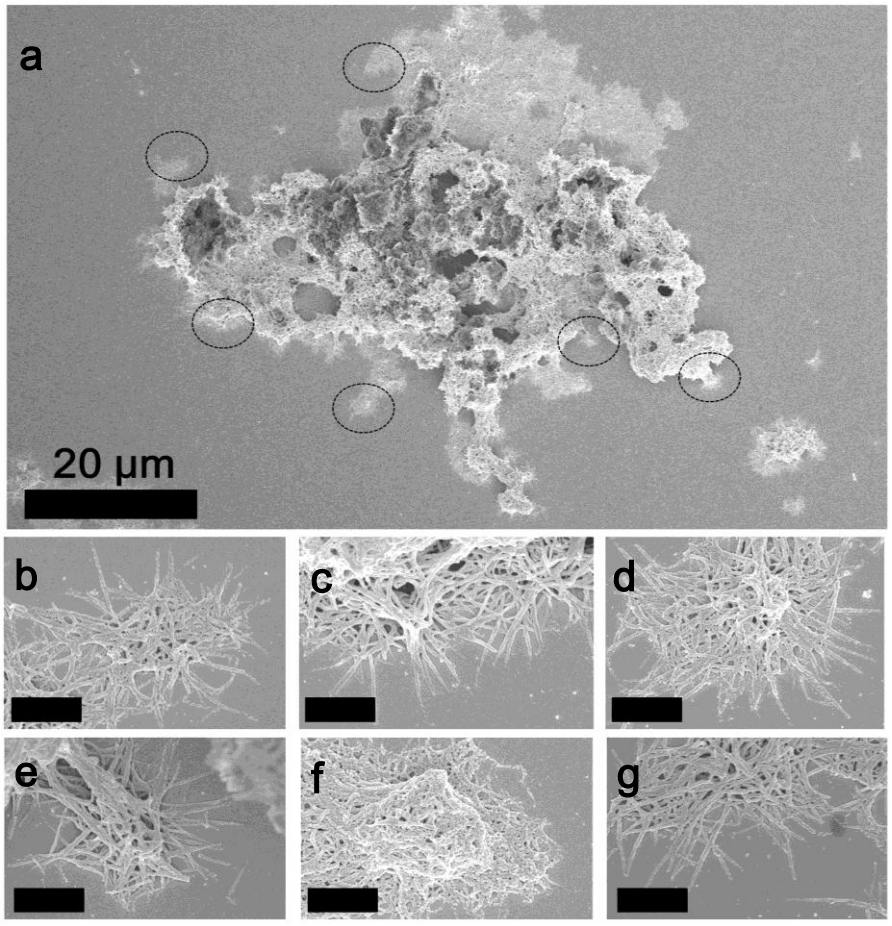

Fig. S4. Homochiral helix network (L-handed). a) Over view of the formed helix network. b-g) Magnified views of different regions noted by the black circles. Bar = 1 μm.

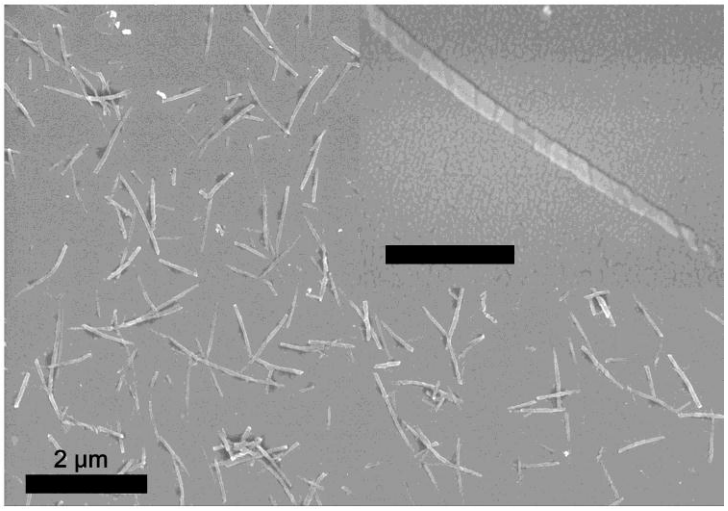

Fig. S5. SEM image of dispersed nano-helixes (KUDOS, 35 KHz). Insert: an isolated nano-helix. Bar = 500 nm. 600 dispersed helixes were counted in five different samples. The amount of L- or R- handed helixes were 297 and 303, respectively.

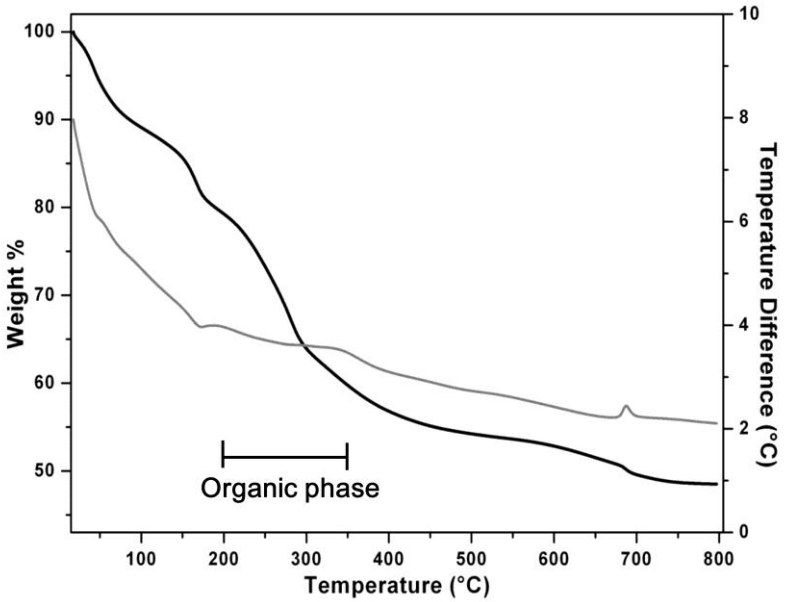

Fig. S6. TGA (dark line) and DSC (light line) results of nano helixes. The organic content was calculated from 200°C to 350°C, while the remains (above 350 ^{o}C) were attributed to the inorganic content. Note: brushite ($CaHPO_4 \cdot 2H_2O$) has two crystal water, which could be lost at temperature of 100-200°C.[1] AOT and BSA could be degraded at temperature below 350°C.[2] Therefore, the weight loss before 200 °C was due to water (including absorbed water and crystal water in the hybrid) and that during 200°C to 350°C was attributed to the organic components.

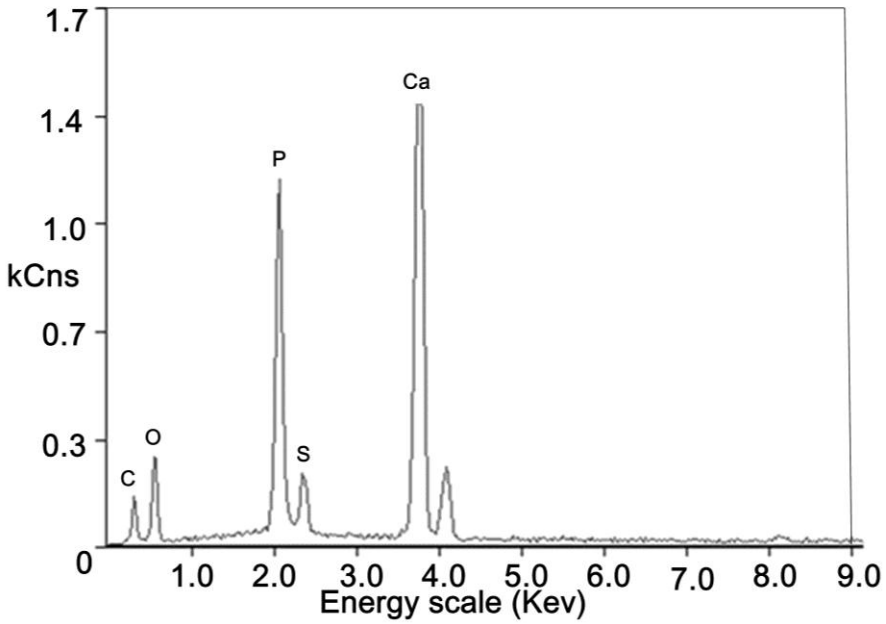

Fig. S7. EDS result of nano-helixes. The presence of elements of carbon, oxygen, phosphorus, sulphur and calcium was shown respectively, which indicate the presence of AOT and calcium phosphate.

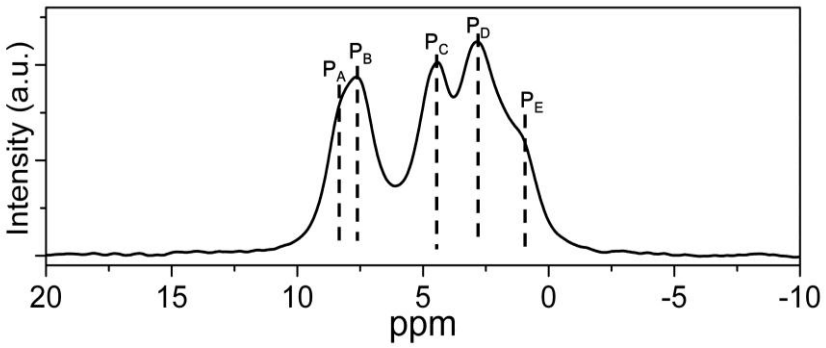

Fig, S8. $^{31}P\{^{1}H\}$CPMAS spectra measured for nano helixes. The spectra was recorded at spinning frequency of 10 kHz and the contact time was set to 2.5 ms. More than four resolved peaks were observed in the spectra, rendering the spectral assignment very difficult. To further characterize the phosphorus environments, a series of $^{31}P\{^{1}H\}$ CPMAS spectra of the two samples and selected model compounds with variable contact times were measured and the signal intensities were analyzed to extract the τ_{cp} and $T_{1\rho}^{H}$ values, as summarized in Table 1. By the comparison of the τ_{cp} values of models and the samples, we concluded that all the phosphorus species belonged to either HPO_4^{2-} or $H_2PO_4^{-}$ environment, in which considerable protons existed in the vicinity of ^{31}P nuclei.

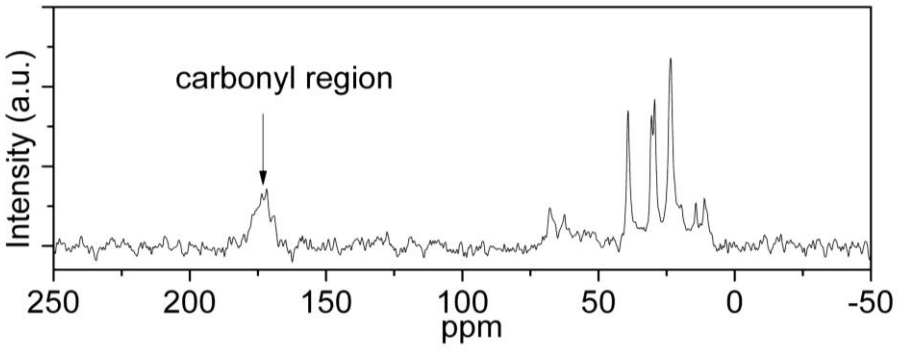

Fig. S9. $^{13}C\{^{1}H\}$CPMAS spectra measured for the nano helixes. The broaden resonance in the carbonyl region indicated that the carbonyl group is crucial in interacting with the minerals, which suggested a tiny amount of absorbed BSA existed.

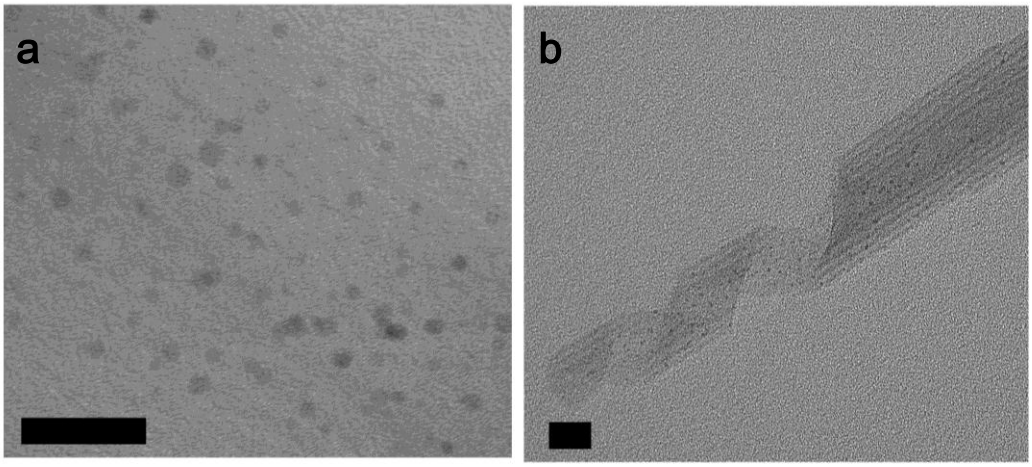

Fig. S10. (a) Synthesized BSA protected Au nanoparticles. The size of Au nanoparticles was between 1-2 nm. (b) Nano-helixes formed by using BSA-Au instead of pure BSA. The tiny dots were BSA protected Au nanoparticles, which preferred to absorbed on the regions of inorganic phase (dark lines). Bars in (a) and (b) is 20nm. We note that the BSA only absorb on the surface of nano-helixes. On one hand, the BSA molecules are hard to be incorporated into the inner structure due to its large dimension (140 x 40 x 40 Å3). On the other hand, the distribution of Au nanoparticles will be homogeneous if it acts as a part of component during the helix formation.

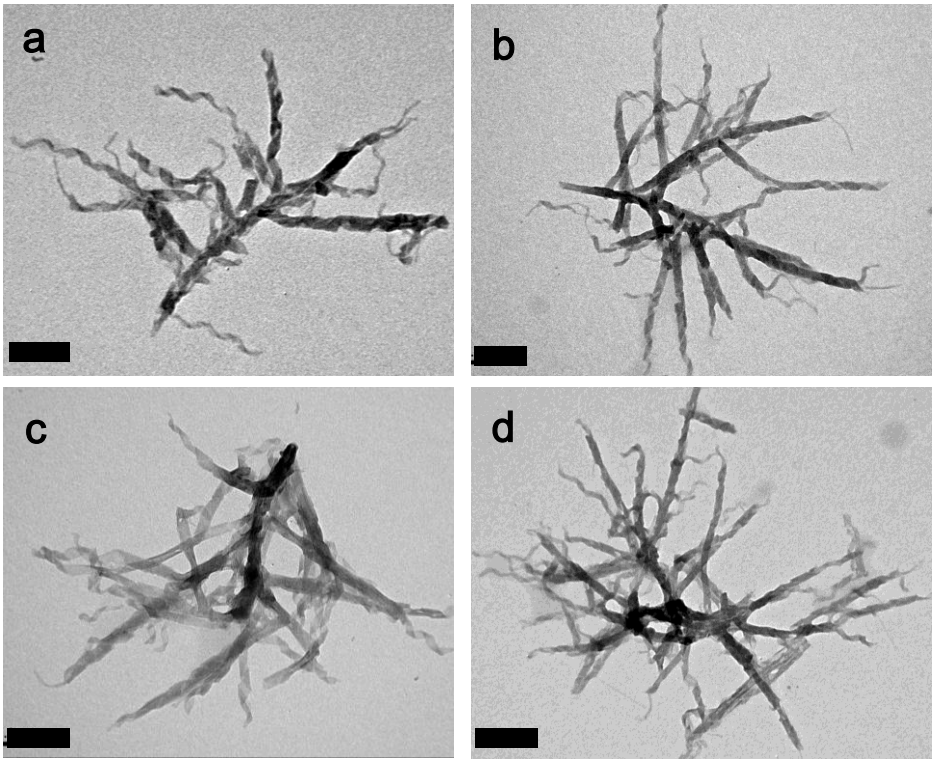

Fig. S11. (a-d). TEM results of seed growth experiment. In the experiment of seed growth, 1/20 percent of obtained product (the complex of nanohelixes, Fig 2 and Fig S2) was underwent intense ultrasonic treatment (KUDOS, 35 KHz, 20 min) and the helix clusters or networks were collapsed into dispersed helixes (Fig. S5). Then the dispersed helixes were added as seeds into freshly prepared reaction solutions and the reaction solutions were collected by centrifugation and observed with Transmission electron microscopy (TEM). The time for forming homochiral helixes formation homochiral helix clusters could be reduced to about 3h. We noted that the time for the formation of helix cluster is reduced and the numerous small clusters quickly form and quickly appeared within 1h to 2h. In comparison, no products form at this stage if no seeds are added. This indicated that mother helix could act as the seed to induce the proliferation of new helix to form homochiral helix clusters, rather than to aggregate helixes into homochiral helix clusters.

2. Tables

Table S1. Summary of NMR data determined for model compounds and nano helixes. The spin-locking field for ^{1}H was set to 50 kHz, while linear ramping was applied in the ^{31}P channel to fulfil Hartman-Hahn matching condition.

Sample	Site	δ_{iso} (ppm)	T_1 (s)	τ_{CP} (ms)	$T_1\rho$ (ms)
Hydroxyapatite $Ca_{10}(PO_4)_6(OH)_2$	P	2.8	n.d.	1.36 ± 0.12	> 50
Brushite $CaHPO_4 \cdot 2H_2O$	P	1.4	n.d.	c.a. 0.5	c.a. 10
Monetite	P_1	-0.3	n.d.	0.33 ± 0.03	34.5 ± 4.4
$CaHPO_4$	P_2	-1.6	n.d.	0.53 ± 0.04	39.5 ± 5.1
Glyphosate $C_3H_8NO_5P$	P	13.1	n.d.	0.29 ± 0.02	45.0 ± 5.5
Nano helixes	P_A	8.5	42	0.97 ± 0.15	6.8 ± 0.8
	P_B	7.7	39	0.64 ± 0.06	6.8 ± 0.6
	P_C	4.3	37	0.83 ± 0.11	8.9 ± 1.0
	P_D	3.0	37	0.75 ± 0.07	9.3 ± 0.8
	P_E	1.2	34	0.77 ± 0.14	9.2 ± 1.4

Note: Error of the chemical shift data is estimated to be 0.1 ppm.

Table S2. Free calcium ion concentration in BSA, AOT and BSA+AOT solutions (200ml).

Items	BSA	AOT	Free [Ca^{2+}]
Blank	0 mg/ml	0 mM	1.25 mM
BSA	0.5mg/ml	0 mM	1.1 mM
AOT	0 mg/ml	0.5mM	0.78 mM
BSA+AOT	0.5 mg/ml	0.5mM	0.62 mM

Note: BSA molecule contains 585 amino acid residues and has a molecular weight of 66463 Da (5539 g/mol). The 100 AOT molecule can bind 94 Ca^{2+} , while 10000 amino acid residues only can bind 28 Ca^{2+}. Thus, AOT molecule is more capable in binding Ca^{2+}.

3. References

1 Dosen, A.; Giese, R. F. *Am. Mineral.* 2011, **96**, 368-373.

2 Omastova, M.; Rychly, J.; Trchova, M.; Kovarova, J. *Des. Monomers Polym.* 2004, 7, 633-646.